Appl Biochem Biotechnol (2016) 178:654–669
DOI 10.1007/s12010-015-1900-z

Detection of Asp371, Phe375, and Tyr376 Influence on GD-95-10 Lipase Using Alanine Scanning Mutagenesis

Renata Gudiukaitė[1] · **Audrius Gegeckas**[1] · **Mikas Sadauskas**[1] · **Donaldas Citavicius**[1]

Received: 20 June 2015 / Accepted: 13 October 2015 /
Published online: 19 October 2015

Abstract GD-95-10 and GD-95-20 lipases are modified GD-95 lipase variants, which lack 10 and 20 C-terminal amino acids, respectively. Previous analysis showed that GD-95-10 lipase has higher activity than GD-95 lipase, while GD-95-20 lipase almost completely loses its activity. Analysis in silico suggested three conservative amino acids at region between 369 and 378 amino acids which can be relevant to the activity of GD-95-10 lipase. These amino acids have direct contacts with residues involved in substrate binding, stabilization of the serine loop or form oxyanion hole. In this work, the role of Asp371, Phe375, and Tyr376 on activity, functionality, and structure of GD-95-10 lipase was analyzed by Ala scanning mutagenesis. We showed that even a single mutation can impact the main structure and activity of *Geobacillus* lipases. Our experiments provide new knowledge about lipases from thermophilic *Geobacillus* bacteria and are important for protein engineering and synthetic biology. These enzymes and their engineering can be basis for future biocatalysts applied in production of biofuel or other industrial esters.

Keywords Biotechnology of thermophiles · *Geobacillus* lipases · C-terminal amino acids · Alanine scanning mutagenesis · Gene cloning and expression · Protein engineering

Introduction

The rapid evolution of bioconversion and ecotechnology strongly increases the focus on the enzymes which possess novel properties. These new enzymes can change the chemical less eco-friendly synthesis of various industrial products. One of the most interesting classes of

Electronic supplementary material The online version of this article (doi:10.1007/s12010-015-1900-z) contains supplementary material, which is available to authorized users.

✉ Renata Gudiukaitė
renata.gudiukaite@gmail.com

[1] Department of Microbiology and Biotechnology, Faculty of Natural sciences, Vilnius University, Čiurlionio 21/27, 03101 Vilnius, Lithuania

enzymes is lipases from *Geobacillus* bacteria, because they can be active at extreme conditions and have a great potential for application in bioconversion and ecotechnology [1]. Lipases are widely applied in the production of pharmaceuticals, leather, detergents, foods, and medical diagnostics [2–6]. The ability to manipulate these lipases and give them new properties depends on the knowledge about the role of their individual domains and amino acids.

Scanning mutagenesis strategies have proven to be a useful approach to structure-function and protein evolution studies [7, 8]. In these experiments, one or several amino acid residues are changed (i.e., to alanine) and the resulting mutant proteins are analyzed for changes in function [9]. Although alanine scanning mutagenesis can be a difficult method, it has been useful for the analysis of interactions at protein–protein interfaces or for the identification of residues involved in substrate recognition [10] or protein stability [11]. The alanine-scanning mutagenesis was successfully applied by Pezzullo et al. to analyze esterase 2 from *Alicyclobacillus acidocaldarius* [12]. Also, Timucin and Sezerman used Trp211Ala and Trp234Ala mutations to investigate the role of Trp211 and Trp234 in thermostability and thermoactivity of bacterial lipases [13].

Previously, we described the influence of N- and C-terminal region on activity, structure, and functionality for GD-95 lipase from *Geobacillus* sp. 95. The bioinformatics analysis of the GD-95 lipase revealed that α13 helix of this lipase has six conserved residues. Most of them (Phe375, Tyr376, Leu379, Ala380, and Leu383) are directed toward the center of a protein and form hydrophobic contacts. The functionality of GD-95 lipase without 10 C-terminal amino acids and loss of activity in GD-95-20 shows that this lipase can successfully function, and the important amino acids from C-terminal-deleted region are located at the region from 369 to 378 amino acids. Three conservative amino acids (Asp371, Phe375, and Tyr376) are located at this region [14]. This provided a basis for further experiments. We decided to create Ala mutants of these amino acids to verify whether contacts formed between these and other amino acids are indeed important for GD-95-10 lipase functionality and which amino acids are responsible for the loss of GD-95-20 lipase functionality. In this study, we have constructed six mutants of GD-95-10 lipase. All of these constructs were cloned into pET-21c(+) vector, expressed in *Escherichia coli* BL21(DE3) cells, purified using IMAC methodology. The yield, activity, and influence of temperature on mutated GD-95-10 lipase activity and stability were evaluated. Also, the analysis of contacts in three-dimensional structure in GD-95-10, GD-95-20, and mutated lipases was performed.

Materials and Methods

Bacterial Strains, Plasmids, and Culture Conditions

E. coli strains DH5α and BL21(DE3) were used in this study. *E. coli* transformants were grown in Luria-Bertani (LB) medium with 100 μg/ml ampicillin at 37 °C with agitation (180 rpm) [15]. Vector pTZ57R/T (Thermo Fisher Scientific) was used as the cloning vector for the mutated lipase gene in *E. coli* DH5α strain and pET-21c(+) (Novagen) for enzyme expression in *E. coli* BL21(DE3). LB agar containing 100 μg/ml ampicillin, 0.5 mM IPTG, 20 μg/ml X-Gal, and 0.5 % emulsified tributyrin (TB) was used to screen the recombinant clones carrying pTZ57R/T plasmids. *E. coli* BL21(DE3) transformants harboring plasmid pET-21c(+) with mutated lipase insert were screened on the same medium without IPTG and X-Gal.

DNA Manipulations and Alanine Mutagenesis

The mutated lipase variants R1–R6 were constructed using primers designed according to GD-95-10 lipase sequence [14]. The primers are listed in Table 1. These following mutated primers were used to substitute the nucleotide sequence coding Asp371, Phe375, and Tyr376 with GCA, coding Ala. Plasmid DNA was extracted from *E. coli* BL21(DE3) transformants GD-95-10 (described in previous study) was used as a template for the PCR amplification of mutated GD-95-10 lipase variants, and amplification process was set up as described previously [14]. After amplification each mutation was confirmed by sequencing. The cloning procedure was carried out according to Gudiukaitė et al. [14]. The resulting plasmid was transformed into *E. coli* DH5α and then retransformed into *E. coli* BL21(DE3) competent cells for expression. Positive clones were identified by lipase activity on plates supplemented with tributyrin and double restriction digestion with *Not*I and *Nde*I.

In Silico Analysis of GD-95-10 Lipase Mutants

Positional variability was assessed by the analysis of sequence logos generated using WebLogo (http://weblogo.berkeley.edu) [16]. The analysis was carried out with sequences, which were used in previous work [14] for multiple sequence alignment. Homologs of GD-95 lipase were found by performing BLAST search against nr70 protein database (nonredundant protein database filtered to 70 % sequence identity). Three-dimensional (3D) structures of GD-95-10 lipase and its R1–R6 mutants were predicted with MODELLERv9.10 program (http://www.salilab.org/modeller/) using an organic solvent tolerant lipase 42 (pdb: 4fkb) as template. Model quality was assessed using ProSA-web server (https://prosa.services.came.sbg.ac.at/prosa.php) [17]. Possible interactions of both mutated and other amino acids important for

Table 1 Summary of the GD-95-10 mutants and primer sequences used for the alanine mutagenesis

Mutant's name	Primer	Sequence	Inserted restriction site
R1	Gelip95-43-F	5′-TGA AGC GCA TAT GGC AGT TTC ACG CGC CAA-3′	*NdeI*
	Rev-10-Tyr376Ala+ Asp371Ala	5′-TAG CGG CCG CCC GCA A**AG C**AA AGG CGC GAA T**AG C**AA ATG-3′	*NotI*
R2	Gelip95-43-F	5′-TGA AGC GCA TAT GGC AGT TTC ACG CGC CAA-3′	*NdeI*
	Rev	5′-TAG CGG CCG CCC GCA A**AG CAG C**GG CG-3′	*NotI*
R3	Gelip95-43-F	5′-TGA AGC GCA TAT GGC AGT TTC ACG CGC CAA-3′	*NdeI*
	Rev-10-Asp371Ala	5′-TAG CGG CCG CCC GCA AAT AAA AGG CGC GAA T**AG C**AA ATG-3′	*NotI*
R4	Gelip95-43-F	5′-TGA AGC GCA TAT GGC AGT TTC ACG CGC CAA-3′	*NdeI*
	Rev-10-Phe375Ala	5′-TAG CGG CCG CCC GCA AAT A**AG C**GG CGC GAA T-3′	*NotI*
R5	Gelip95-43-F	5′-TGA AGC GCA TAT GGC AGT TTC ACG CGC CAA-3′	*NdeI*
	Rev-10-Tyr376Ala	5′-TAG CGG CCG CCC GCA A**AG C**AA AGG CGC G-3′	*NotI*
R6	Gelip95-43-F	5′-TGA AGC GCA TAT GGC AGT TTC ACG CGC CAA-3′	*NdeI*
	Rev-10-Phe375Ala+ Asp371Ala	5′-TAG CGG CCG CCC GCA AAT A**AG C**GG CGC GAA T**AG C**AA ATG-3′	*NotI*

Sequences underlined indicate the restriction sites and sites of mutations are double underlined in bold

functionality of *Geobacillus* lipases were analyzed using CAD-score (http://bioinformatics.ibt.lt/cad-score/) [18]. The distances between catalytic amino acids and other important residues were calculated using RasMol (http://rasmol.org/).

Expression and Purification of Mutant Proteins

Establishment of the conditions for expression of GD-95-10 lipase mutants was performed according to Gudiukaitė et al. [14]. The localization of mutant lipases was detected by analyzing soluble and insoluble fractions of proteins in SDS-PAGE [19]. Cells were harvested by centrifugation (8000*g*, 15 min), when maximum amount of expressed lipases was detected. Cells were suspended in binding buffer (50 mM Tris–HCl, pH 8.0), placed on ice and disrupted by sonication. After centrifugation (20,000*g*, 15 min), the resulting supernatant was tested as soluble proteins and cell debris dissolved in 50 mM Tris–HCl buffer (pH 8.0) with 6 M urea—as inclusion bodies. The purification in details of GD-95-10 lipase and its mutants for native conditions was according to previous work performed in our laboratory [14]. The GD-95-10 lipase mutants were purified using immobilized nickel ion affinity chromatography (Profinity™ IMAC Resins, BIO-RAD) as described in the manufacturer's purification protocol with minimal modification. In this process, 50 mM Tris–HCl, pH 8.0 was used as binding buffer and the same buffer with 6 M urea and 10 and 250 mM imidazole—as wash and elution buffers, respectively.

Protein concentration and SDS-PAGE analysis was carried out as described in Gudiukaitė et al. [14].

Determination of Lipase Activity

The lypolitic activity in zymogram after SDS-PAGE was detected used trybutirin as substrate. Lipolytic activity was measured spectrophotometrically using *p*-nitrophenyl (*p*NP) dodecanoate (Sigma-Aldrich) as a substrate according to previous work [14]. One unit of lipase activity was defined as the amount of enzyme that releases 1.0 μmol of *p*-nitrophenol from the substrate per minute.

Kinetic Analysis

The Michaelis–Menten constant (K_m) and the maximum velocity for the reaction (V_{max}) as well as K_{cat} were calculated using *p*NP laurate (*p*NPL) as substrate at concentrations ranging from 1.25 to 50 mM. The temperature, pH, and quantity of the enzyme were kept the same as for the enzyme activity assay described above. Lineweaver–Burk plots were used to determine V_{max} and K_m parameters, assuming that the reactions followed a simple Michaelis–Menten kinetics.

Detection of Temperature Optimum and Thermostability

The optimal temperature for activity of GD-95-10 lipase mutants was determined by the lipase assay at temperatures ranging from 5 to 80 °C. Due to instability differences of *p*NP dodecanoate at different temperatures, the reaction mixture used as a control was parallely incubated at the given temperature without enzyme solution. The effect of temperature on GD-95-10 lipase mutants' stability was investigated by measuring the residual activity at 55 °C after GD-95-10 lipase mutants were incubated at 30–80 °C for 30 min [14].

Statistical Analysis

All experiments were repeated three times, and the average means were derived. Standard deviation from the mean is shown in Table 2 and Fig. 4. Significant differences between lipases were calculated using two-sample *t* test (http://in-silico.net/tools/statistics/ttest; α=0.05). Only the results with two-tailed *p* value less or equal to 0.02 are presented in this paper.

Results and Discussion

Selection of Mutagenesis Sites

Previous analysis in silico has shown that Asp371, Phe375, and Tyr376 are conservative amino acids and play important role in activity of GD-95 lipase (GenBank KC609753.1) [14]. The following analysis in WebLogo (Fig. 1) also suggested that these amino acids are important for lipolytic activity. In WebLogo analysis, the overall height of each stack indicates the sequence conservation at that position (measured in bits), whereas the height of symbols within the stack reflects the relative frequency of the corresponding amino acid or nucleotide at that position. Sequence logos provide a richer and more precise description of sequence similarity than consensus sequences and can rapidly reveal significant features of the alignment [16]. The major focus has been given on the region between 369 and 378 amino acids, because the GD-95-10 lipase was fully functional. In this region, positions 371, 372, 375, and 376 are partially buried, and therefore tend to be populated by hydrophobic amino acids Leu, Phe, and Tyr. We decided to mutate three amino acids Asp371, Phe375, and Tyr376 to Ala and evaluate the role of these amino acids on GD-95-10 lipase functionality and structure. The schematic presentation of the generated variants is shown in Fig. 2.

Table 2 Yield and activity of GD-95-10 lipase mutants R1-R6 and GD-95-20 lipase

Protein	Size of clear zones around *E. coli* BL21(DE3) transformant colonies. High (+++), very small (+), not detectable (−)	Yield (mg) of expressed protein from 200-mL culture (soluble fraction)	Specific activity (U/mg)	Author
GD-95-10	+++	9.52	415.00	[14]
GD-95-20	−	3.95	14.00	[14]
R1 (Asp371Ala+Tyr376Ala)	−/+	3.20	12.52	This study
R2 (Phe375Ala+Tyr376Ala)	−/+	5.33	11.67	This study
R3 (Asp371Ala)	+	9.79	15.50	This study
R4 (Phe375Ala)	++	5.43	42.50	This study
R5 (Tyr376Ala)	−/+	6.05	32.50	This study
R6 (Asp371Ala+Phe375Ala)	−/+	2.93	20.00	This study

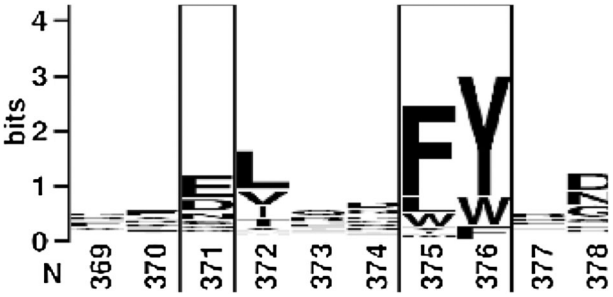

Fig. 1 Sequence logos of GD-95 lipase region between 369 and 378 amino acids generated used WebLogo server. Overall height of each stack indicates the sequence conservation at that position (measured in bits), whereas the height of symbols within the stack reflects the relative frequency of the corresponding amino acid at that position [16]. In this work, the WebLogo analysis was carried out with lipase sequences, which were used for multiple sequence alignment in previous work [14]. The mutated amino acids are marked in *box*

Expression, Purification, Activity, and Yield Analysis of six GD-95-10 Lipase Mutants

pET-21-lip-mut plasmids, created by cloning genes coding lipase mutants into pET-21c(+), were transformed into *E. coli* BL21(DE3) cells and protein expression from transformants containing R1–R6 constructs was monitored and analyzed by SDS-PAGE (Fig. 3). SDS-PAGE analysis showed the appearance of a large amount of new protein in *E. coli* BL21(DE3) cell sample after induction with IPTG. The size of this newly expressed protein agreed well with the predicted size of GD-95-10 lipase mutants (approximately 43 kDa). Results of zymographic analysis are shown in Fig. 3d. The

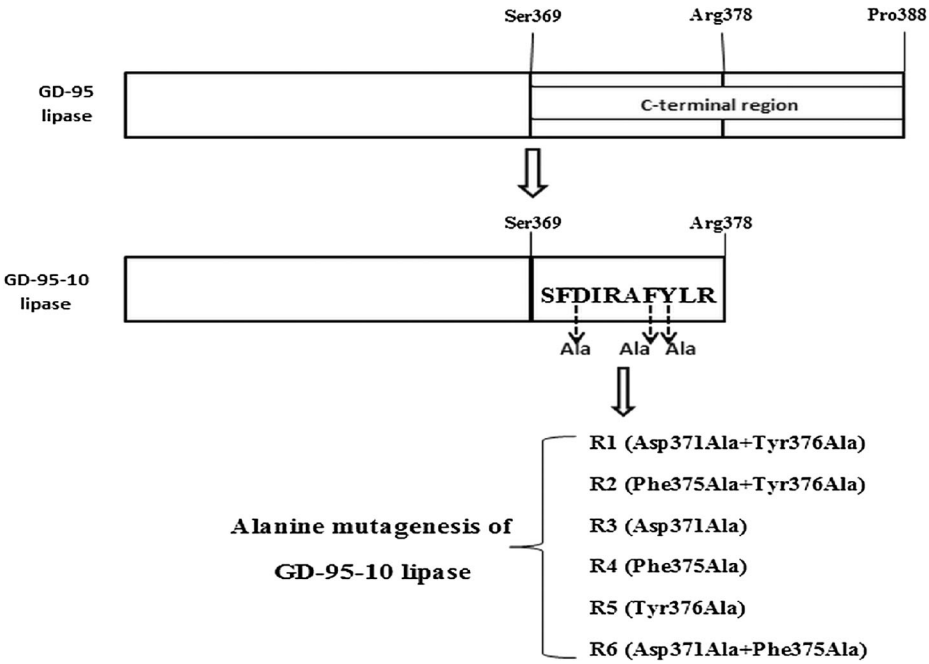

Fig. 2 Schematic presentation of generated R1-R6 constructs

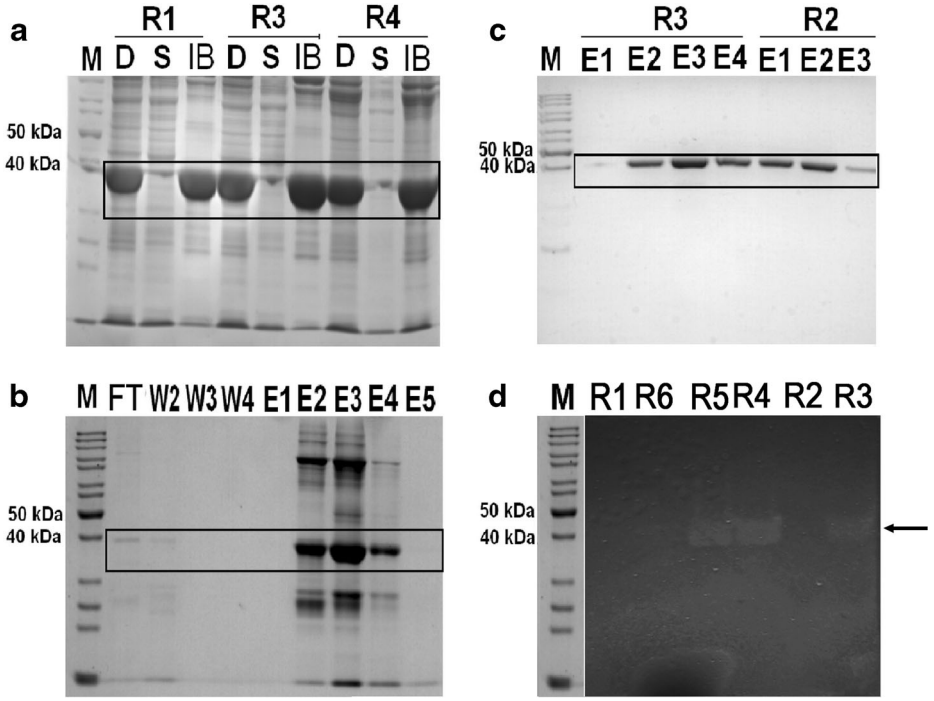

Fig. 3 SDS-PAGE (12 %) analysis of recombinant R1-R6 lipase mutants. M- PageRuler™ Unstained Protein Ladder. Analysis of soluble and insoluble fraction of R1, R3, and R4 lipase mutants (**a**): *D* sample after sonication, *S* soluble proteins, *IB* inclusion bodies. Purification of R4 lipase mutants from inclusion bodies using IMAC for denaturating conditions (**b**): *FT* flow through, *W2-W4* washing fraction, *E1-E5* elution fraction. Purification of R3 and R2 lipase mutants from soluble protein sample using IMAC for native conditions (**c**): *E1-E3* elution fraction. Zymogram of R1-R6 lipase mutants cells sample after induction (**d**). The *boxes* (**a**–**c**) and the *arrow* (**d**) indicate the location of the target lipases

optimum expression of R1–R6 mutated lipases was detected at 2 h post-induction with 1.0 mM IPTG. The same results were achieved with GD-95 lipase and its modified constructs [14]. All six Ala mutants of GD-95-10 lipase were cloned without signal peptide, based on our previously described results [14] and other literature references [20, 21], suggesting that removal of the N-terminal signal peptide significantly enhances the yield of *Geobacillus* lipases. Analysis of soluble and insoluble proteins in protein sample after transformant cells disruption by sonication was carried out for initial purification of R1–R6 mutants (Fig. 3a). Protein analysis showed that R1–R6 lipases form inclusion bodies and the largest amount of proteins are in insoluble fraction. These results suggested that Asp371, Phe375, and Tyr376 mutation to Ala increased aggregability of GD-95-10 lipase. Assuming that aggregability of GD-95-10 lipase is 0 %, the aggregability of R mutant increased 30 % (comparing the protein amount in the elution fractions after purification from the same culture volume under native and denaturating conditions). Since mutated proteins after purification in denaturating conditions showed very low activity (about 0.12 U/mg) and the protein samples were nonhomogeneous (Fig. 3b) and affected by urea, we used the soluble fraction of all mutated lipases for further experiments. The purification of R2 and R3 mutants in native conditions is presented in Fig. 3c.

Our results showed that all mutations strongly decreased the yield and activity of GD-95-10 lipases (Table 2). This might be explained by the fact that mutations significantly changed the distances and possible contacts between amino acids, which are responsible for the catalytic activity or binding of substrate (Tables S2 and 4, Fig. 6).

Double Asp371Ala+Tyr376Ala (R1 lipase) and Phe375Ala+Asp371Ala (R6 lipase) mutations resulted in the most significant changes not only in the yield of GD-95-10 lipase but also in the lipolytic activity (Table 2). The yield of these mutants was similar to the yield of GD-95-20 lipase and three times lower than GD-95-10 lipase. R1 and R6 lipases retained only 3 and 5 %, respectively, lipolytic activity of GD-95-10 lipase. Since R3 mutant had the lowest lipolytic activity among all single mutants, we predict that Asp371 has decisive influence in double mutants. R3 mutant retained only 4 % of lipolytic activity compared to GD-95-10 lipase. According to previous analysis [14], Tyr376 makes the most important contacts with other amino acids in GD-95-10 lipase, but single Tyr376 mutant possesses 32.5 U/mg specific activity and this activity is higher than all double mutants as well as Asp371Ala. Therefore we argue that both Asp371 and Tyr376 play the largest role in GD-95-10 lipase activity and together in inactivation of GD-95-20. Substitution of these residues can be the reason why GD-95-20 lipase is not functional. The single mutation of aromatic acids Phe375 and Tyr376 to Ala decreased activity of GD-95-10 lipase by 85 and 89 %, respectively, but this activity was still detectable on agar medium with tributyrin which suggests that this mutation was not as critical as Asp371Ala+Phe375Ala, Asp371Ala+Tyr376Ala, and Phe375Ala+Tyr376Ala double mutations.

Kinetic Analysis of Six GD-95-10 Lipase Mutants and Its Predecessors

Catalytic constants (V_{max}, K_{cat}, K_m, and catalytic efficiency) were calculated in order to evaluate the effect of mutations on lipolytic activity of GD-95-10 mutants. R4 mutant clearly distinguished from all GD-95-10 lipase derivatives as they possessed very high K_m values when *p*NPL was used as a substrate. This mutant has Phe375Ala mutation, suggesting that Phe375 is also important for GD-95-10 functionality. Interestingly, R3 mutant possessed the lowest K_m value among all mutants with *p*NPL as a substrate. This means that R3 mutant has a higher affinity for *p*NPL although it has a low lipolytic activity. This can be explained by the fact that *p*NPL can be bound by the enzyme; however, catalysis is not effective. Kinetic analysis also showed that GD-95-10 derivates had very low V_{max} compared with GD-95 and GD-95-10 lipases in the case with *p*NPL. R1, R2, R3, and R5 mutants had the lowest V_{max} values, while R1 lipase, which is Asp371 and Tyr376 mutant and R5 mutant, possessed the lowest K_{cat} and catalytic efficiency values with *p*NPL. The K_{cat} and catalytic efficiency values of R5 mutant are 60 and 7.2/min/mM, respectively. The higher the K_{cat}/K_m, the better the enzyme works on that substrate. GD-95 and GD-95-10 lipases possessed the highest values. This kinetic analysis of mutants confirmed hypothesis that Asp371 and Tyr376 are the most important amino acids from C-terminal end of GD-95-10 lipase. Detailed analysis of kinetic parameters of mutated lipases is presented in Table 3. Therefore, we conclude that Phe375 is very important for interaction with substrate but Asp371 and Tyr376 also play significant role in lipase activity and catalytic efficiency control.

Influence of Ala Mutation on Temperature Activity and Stability of R Mutants

The effect of a single amino acid mutation on GD-95-10 lipase temperature activity and thermostability was investigated using R3–R5 mutants. Analysis showed that Asp371Ala

Table 3 Kinetic properties of mutated GD-95-10 lipase variants, GD-95, GD-95-10 and GD-95-20 lipases

Kinetic parameters Protein	V_{max} (μmol/min mg protein)	K_m (mM)	K_{cat} (/min)	Catalytic efficiency K_{cat}/K_m (/min/mM)
GD-95	58.82	7.69	2.56×10^3	3.33×10^2
GD-95-10	50.00	8.33	2.83×10^3	3.40×10^2
GD-95-20	40.00	7.70	1.67×10^2	2.16×10
R1 (Asp371Ala+Tyr376Ala)	3.03	16.67	1.26×10^2	8.00
R2 (Phe375Ala+Tyr376Ala)	5.26	12.50	2.08×10^2	16.64
R3 (Asp371Ala)	5.61	6.67	2.34×10^2	35.00
R4 (Phe375Ala)	20.00	25.00	8.33×10^2	33.00
R5 (Tyr376Ala)	1.43	8.33	60.00	7.20
R6 (Asp371Ala+Phe375Ala)	ND	ND	ND	ND

The values were determined at 55 °C using *p*NP laurate as substrate

mutant (R3) displays a very close temperature profile for GD-95-20 and GD-95-10 lipases. Also, the temperature optimum for R3 lipase activity was lower than GD-95-10 and GD-95-20 lipases (40 °C) (Fig. 4a), but R3 lipase retained its lipolytic activity up to 70 °C. R4 lipase mutant had the same temperature optimum. Also, the activity of R4 lipase mutant strongly decreased at 60 °C (approximately 20 % residual lipolytic activity). This difference from other lipases is significant with p value 0.02. R5 mutant significant differences are not shown. R3 mutant showed the lowest thermostability compared to both GD-95-10 and GD-95-20 lipases and other R mutants (Fig. 4b). This suggests that Phe375 might be the most important for lipase activity at higher temperature, while Asp371 plays the major role in stabilization. It appears that constructs of lipases capable of working at higher temperatures possess lower thermostability than lipases, which have narrower temperature range (unpublished results). This feature is also displayed by R3 and R4 mutants.

The inverse correlation between temperature range and stability was also predicted in R2 mutant (Fig. 4c, d), which possesses about 20 % lipolytic activity at 75 °C compared to GD-95-10 lipase, but after 30 min at 60 °C, loses its activity completely. The double GD-95-10 lipase mutant R1 had distinguishable feature of retaining 100 % enzymatic activity at 30–65 °C (Fig. 4c). This is significant with p value 0.02 at 30 °C for GD-95-10 and 0.01 for GD-95-20; 0.01 only for GD-95-10 at 40 °C; and 0.0007 at 65 °C for both GD-95-10 and GD-95-20 lipases. R2 and R6 mutants displayed opposite characteristics: R6 mutant showed lower relative lypolitic activity compared with others mutants at 60–65 °C while R2 mutant worked better at higher temperature (70–75 °C). The differences of R6 with GD-95-10/GD-95-20 are significant with p-value 0.01 at 40 and 60 °C as well as with p value 0.005 at 65 °C. R1 and R6 mutants had very similar capabilities of working at higher temperature. Both these lipases had mutation of Asp371 and are double mutants. These results show that more than a single amino acid is responsible both for the functionality of GD-95-10 lipase and for the inactivation of GD-95-20 lipase, which rather is a consequence of the loss a few amino acids, leading to the changes in the main structure of GD-95-10 lipase.

The substrate specificity and pH optimum of R1–R6 lipases were also analyzed in this study, but significant differences between these lipases were not observed (data not shown).

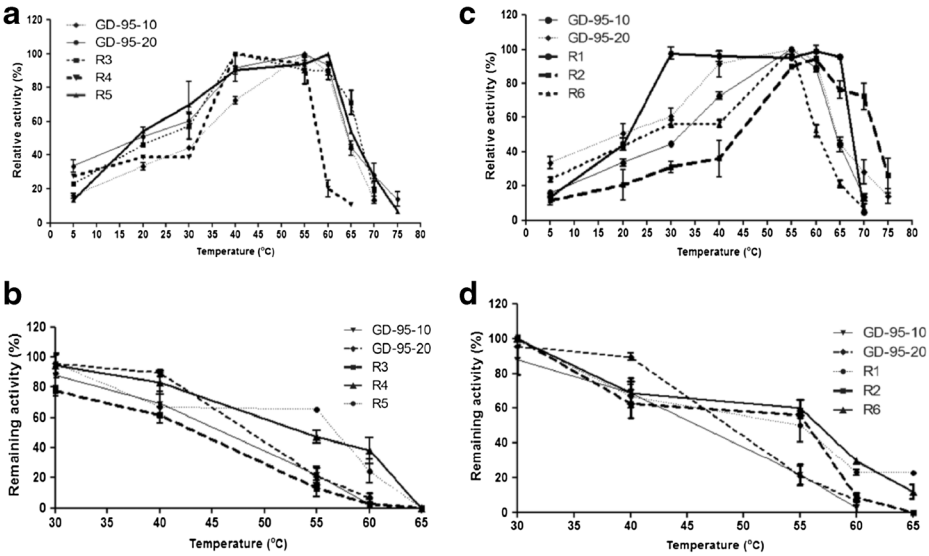

Fig. 4 Effect of temperature on the activity (**a**, **c**) and stability (**b**, **d**) of purified GD-95-10 and GD-95-20 lipases and GD-95-10 lipase mutants R1–R6. Effect of temperature on the activity R3, R4, and R5 mutants (**a**): *thin straight line with a circle*, GD-95-20; *thin dotted line with rhombus*, GD-95-10; *thin dashed line with squares*, R3; *thin dotted line with triangle*, R4; *thick straight line with triangle*, R5. Effect of temperature on the stability of R3, R4, and R5 lipase mutants (**b**): *thin straight line with triangle*, GD-95-10; *thick dashed line with rhombus*, GD-95-20; *thick dotted line with squares*, R3; *thick straight line with triangle*, R4; *thin dotted line with circle*, R5. Effect of temperature on the activity of R1, R2, and R6 mutants (**c**): *thin straight line with hollow circle*, GD-95-10; *thin dotted line with rhombus*, GD-95-20; *thick straight line with circle*, R1; *thick dashed line with squares*, R2; *thick dotted line with triangle*, R6. Effect of temperature on the stability of R1, R2, and R6 lipase mutants (**d**): *thin straight line with triangle*, GD-95-10; *thin straight line with rhombus*, GD-95-20; *thin dotted line with circle*, R1; *thick dashed line with squares*, R2; *thin dotted line with triangle*, R6. Assays for detection of optimal temperature were performed at various temperatures (5–80 °C) under lipase assay conditions. The remaining activity was assayed under lipase assay conditions after the purified recombinant lipases had been incubated at the indicated temperature (30–70 °C) for 30 min. Specific activities of 415.1 U/mg (GD-95-10), 13.9 U/mg (GD-95-20), 12.52 U/mg (R1), 10.71 U/mg (R2), 14.99 U/mg (R3), 60 U/mg (R4), 30.67 U/mg (R5), and 7.2 U/mg (R6) were recorded as 100 %

Analysis of the Contact Changes in Three-Dimensional Structure of R Mutants

To understand the effects of mutated residues to overall structure of GD-95-10 lipase and explain the experimental results, we used in silico methods to obtain structures of mutants and evaluate their contact differences with neighboring amino acids. The 3D structure of GD-95-10 lipase and labeled catalytic and our mutated amino acids from C-terminal end are presented in Fig. 5. The 3D structure quality of GD-95-10 and R1-R6 lipases was predicted using ProSa-web server (Table S1). R1 and R3 mutants had the lowest value from R group mutants. Both these lipases are D371Ala mutants. R1 also has Tyr376 mutation. This suggested that both Asp371 and Tyr376 from C-terminal amino acids are important for GD-95-10 lipase stability and functionality.

Previous analysis in silico suggested that Tyr376 formed the most important contacts from C-terminal region [14]. In GD-95-10 lipase, this amino acid has a direct connection with Leu12 (residue of oxyanion hole [22]), His112 (amino acid from AHSQG pentapeptide, which in the closed state, helps packing catalytic serine and is involved in stabilization of the serine loop [23]), and Ile362 (involved in active site cleft and in acyl chain-binding pocket [23]) (Table S2). Tyr376 mutation to Ala results in complete loss of these contacts (Table S2). This

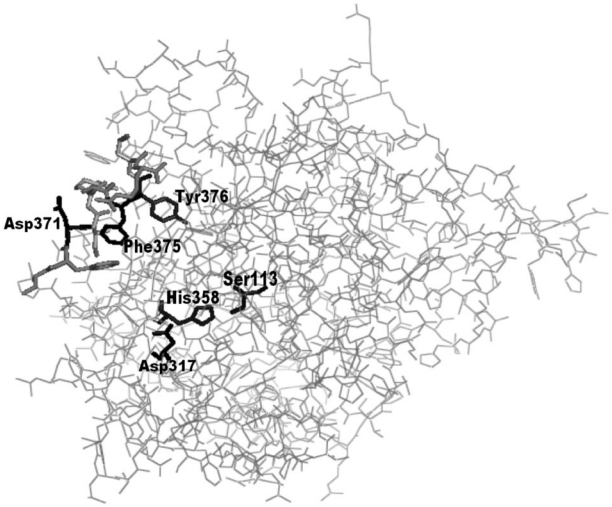

Fig. 5 3D structure of GD-95-10 lipase. The structure predicted with MODELLERv9.10 program and image was generated using Pymol (DeLano Scientific, Palo Alto, CA, USA). The general structure of GD-95-10 lipase is shown in *gray lines*. The residues of 369–378 regions are marked in *gray sticks*; the catalytic residues Ser113, Asp317, His358, and mutated amino acids from C-terminal end are marked in *black sticks*

might explain the activity differences between R1 and R3 mutants since R1 lacks contacts between amino acids in active site cleft and oxyanion hole. The oxyanion hole is an important structure for stabilization of the tetrahedral intermediate during the hydrolysis reaction [23]. The situation is the same in case of R2 mutant. R1 and R2 mutants also lack contacts between Arg34, which interacts with Leu33, involved in formation of channel leading toward the active site [24] and Asp371 (Table S2).

In order to characterize the differences in the main structure of constructed mutants and distance changes between neighboring residues more thoroughly, we carried out contact analysis of amino acids conservative in *Geobacillus* lipases. The results are presented in Table S2. Catalytic His is located at position 358. Contact differences at this position were predicted in R1 mutant. In this mutant connections between catalytic His358 and Asn288, Ser291 and Gly318 are not established (Table S2). R2 and R3 mutants lack contacts between Asp317 and Ser291 while these contacts are present in GD-95-10 and other mutants. To date, the importance and role of Asn288, Ser291, and Gly318 on activity and functionality of *Geobacillus* lipases have not been shown and this is an object for future research.

The analysis of neighboring amino acids also shows that in R6 mutant contacts between His358 and Tyr29 (active site cleft [22]) are lost. Contact analysis may also explain the low stability of R2 lipase. It is possible that this lipase lacks contact between the Ala240, which is involved in active site cleft and Arg62, which plays stabilizing role during lid opening (Table S2). These rearrangements of 3D structure influence the binding of substrate and stability/activity of lipases. Our results suggest that mutations of C-terminal amino acids can affect the interactions between catalytic amino acids and its neighboring residues, and therefore modulate the lipolytic activity of *Geobacillus* lipases.

We also simulated distance changes between catalytic amino acids and several amino acids involved in formation of active site cleft or acyl chain-binding (Phe290; Ile359, Leu12, Phe16, Val187, Gln114, Tyr29) in mutated lipase structures (Table 4, Fig. 6). Residues for this analysis were selected on the basis of contact analysis presented in Table S2. Our results showed that Asp371Ala, Phe375Ala, and Tyr376Ala mutations dramatically changes the distance between catalytic Ser113, Asp317, and His358 (Fig. 6). The distance between catalytic residues of

Table 4 Distance between several important amino acids (without catalytic triad) in GD-95-10 and its mutated variants

		Protein							
		GD-95-10	R1	R2	R3	R4	R5	R6	GD-95-20
Amino acid positions	Phe290-Ile319	12.29	4.20	8.81	4.92	5.25	5.81	7.52	6.92
	Phe290-Ile359	11.81	5.49	10.67	4.46	8.58	4.48	4.36	9.99
	Leu12-Tyr376 or Leu12-Ala376	6.09	6.74	8.50	4.98	6.63	8.44	6.40	-
	Phe16-Val187	11.96	12.82	13.03	12.53	12.61	12.30	12.81	8.53
	Gln114-Ser57	9.39	10.00	10.18	10.61	11.59	7.24	8.57	10.46
	Phe16-Tyr29	11.49	11.98	12.15	10.96	11.96	11.54	11.33	6.89

The distances are presented in Å. The calculation was carried out using 3D structures of each mutant predicted with MODELLERv9.10 program

Geobacillus lipases (Ser113, Asp317, and His358) and its contacts with other amino acids are very important for the catalytic activity of lipases [25]. Goodarzi with colleagues showed that distances between catalytic Asp317-His358 and His358-Ser113 are 5.31 and 1.85 Å, respectively [26]. Other authors suggested that in the active state, the serine side chain O_γ atom is 2.96 Å away from the catalytic histidine Nε2 atom, and between His358 and Asp-317 in both closed and open states, the distances are 2.68 and 2.81 Å, respectively [23]. Distances in GD-95-10 lipase between these catalytic amino acids are 5.72 and 2.69 Å (Fig. 6a). These values are similar to the literature data. Analysis of mutated GD-95-10 lipase variants showed that in all mutants the distance between catalytic Ser113 and His358 increased nearly twofold. The highest differences were observed in R2 and R4 mutants, which have Phe375 mutation. The distances in these mutants were 5.31 and 5.11 Å, respectively (Fig. 6d, f). This correlated with experimental results, which showed that lipolytic activity of R4 lipase mutant significantly decreased at 60 °C, and also, these mutants had a higher K_m. Analysis in silico confirmed hypothesis that Phe375 is important for modulation of lipase activity at higher temperature. Abdul Rahman and et al. demonstrated that efficiency of the catalysis process greatly depends on this critical distance. In their study they found that distances between catalytic Ser113 and His358 are affected by the change in temperature. At 80 °C, the distance between catalytic Ser113 and His358 was longer (5.75 Å) compared to that at 70 °C (2.62 Å) which is the optimal temperature of T1 lipase [25]. We found a similar trend in distance changes after Asp371, Phe375, and Tyr376 mutation to Ala (Fig. 6). Therefore, Asp37Ala, Phe375Ala, and Tyr376Ala mutations significantly influence the main structure of lipase and lead to inactivation.

It has also been predicted that catalytic Ser is in tight side chain packing with some residues of the active site (His112, Phe16, Ile319, Thr269, and Met325), and this leads to the stabilization of the serine loop and lipase thermostability [27]. We decided to analyze distance between several amino acid pairs (Phe290-Ile319, Phe290-Ile359, Phe16-Val187, Phe16-Tyr29, and Gln114-Ser57). The highest differences were calculated between Phe290 and Ile359 in R1, R3, R5, and R6 mutants (Table 4). The distance between these amino acids decreased twofold or more (Table 4). These amino acids are involved in acyl chain-binding pocket. Reduced lipolytic activity in R group mutants might be a result of alterations in substrate-binding site as indicated by distance difference between catalytic Ser and residues near the active site.

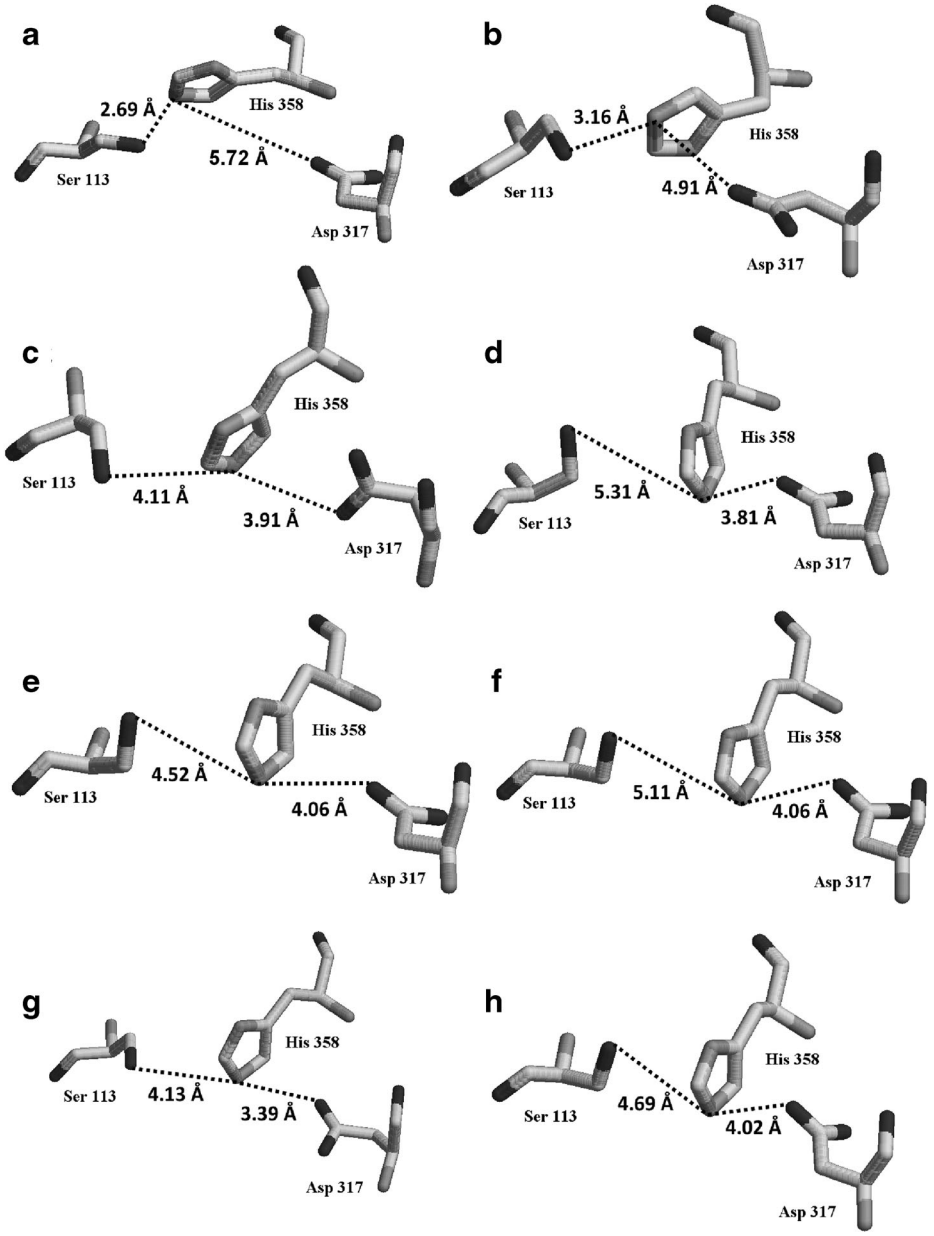

Fig. 6 Iliustration of catalytic triad of *Geobacillus* lipases consisting of Ser113, Asp317, and His358 in GD-95-10 lipase and its mutated derivatives: GD-95-10 (**a**), GD-95-20 (**b**), R1 (**c**), R2 (**d**), R3 (**e**), R4 (**f**), R5 (**g**), and R6 (**h**). The illustration was generated using RasMol (http://rasmol.org/)

CAD-score analysis and also distance differences between catalytic amino acids in R1-R6 mutants supports the hypothesis that mutation of desirable amino acids to Ala changes contacts in lipase structure between amino acids involved in conservative peptide, oxyanion hole, lid domain, active site cleft, and other structural features.

Thus, mutation of C-terminal amino acids affects the general structure of *Geobacillus* lipases. Although changes are minimal, they may be related with the functionality of lipases. The most significant differences in contact area were predicted in R1, R2, R3, and R6 mutants. They are all double mutants and the Asp371 single mutant. These results and experimental data suggested that the most important amino acids for GD-95-10 lipase functionality are Tyr376 and Asp371, but the inactivation of GD-95-20 lipase is a consequence of the removal of all three amino acids, since Phe375 plays significant role in modulation of catalytic activity.

Experimental results and analysis in silico discussed in this study are significant for understanding the relationships between *Geobacillus* lipases' structure and function. Our data suggests that even a single amino acid mutation can affect not the only interactions between important residues, but also lead to the changes in the main structure of lipases. This information is valuable for future modulation of activity and functionality of new lipases for industrial application.

Conclusion

GD-95-10 lipase is a modified variant of GD-95 lipase that is fully functional, while GD-95-20 lipase completely loses its activity. Previous analysis raised the hypothesis that Asp371, Phe375, and Tyr376 are important for GD-95-10 lipase functionality and removal of these amino acids is one of the causes why GD-95-20 lipase loses lipolytic activity. According to the results of in silico analysis, Tyr376 has the most important contacts with other amino acids, which are significant for functionality of *Geobacillus* lipases. In this work, we also show that Asp371Ala mutation (R3 mutant) makes the highest influence on GD-95-10 lipase activity from all single mutations tested and also decreases the temperature optimum and thermostability of GD-95-10 lipase. The thermostability of R3 mutant corresponds to GD-95-20 lipase. The double mutation of Asp371 and Tyr376 to Ala strongly affects the lipolytic activity, yield, and catalytic efficiency of GD-95-10 lipase. These results confirm the hypothesis that the most important amino acids from our mutated C-terminal amino acids are Asp371 and Tyr376, although F375A mutation is also important for GD-95-10 lipase functionality and modulation of catalytic activity. Our analysis shows that three amino acids analyzed in this study influence temperature activity and stability as well as the lipolytic activity and yield of GD-95-10 lipase, but not substrate specificity or pH optimum. Analysis in silico also argue that Asp371, Phe375, and Tyr376 mutation to Ala changes the connections not only between mutated amino acids in 3D structure of GD-95-10 lipase but also the interaction areas and distances between amino acids, which are involved in formation of active site cleft, oxyanion hole or form catalytic triad. Therefore, the loss of activity in GD-95-10 lipase without ten C-terminal amino acids (GD-95-20) does not depend on a single amino acid, but rather is a consequence of the removal of all three amino acids. Results discussed in this paper are valuable for upcoming future modulations of activity and functionality of new lipases and for creation of new enzymes for bioconversion and eco-friendly technologies. These and similar research are not only significant for improving the knowledge about relationships between lipases' structure and functions but also extends our comprehension about naturally existing and biologically active enzymes from *Geobacillus* bacteria.

Acknowledgments This work was supported by the MITA (Agency of Science, Innovation and Technology) program "Development of industrial biotechnology in Lithuania 2011-2013," project "Innovative tools for cosmetic industry (COSMETIZYM)," Grant No. MITA 31V-18.

References

1. Sangeetha, R., Arulpandi, I., & Geetha, A. (2011). Bacterial lipases as potential industrial biocatalysts: an overview. *Research Journal of Microbiology, 6*(1), 1–24.
2. Jaeger, K. E., & Reetz, M. T. (1998). Microbial lipases form versatile tolls for biotechnology. *Tibtech, 16*, 396–403.
3. Bornscheuer, U. T. (2002). Microbial carboxyl esterases: classification, properties and applications in biocatalysis. *FEMS Microbiology Reviews, 26*, 73–81.
4. Singh, R., Gupta, N., Goswami, V. K., & Gupta, R. (2006). A simple activity staining protocol for lipases and esterases. *Applied Microbiology and Biotechnology, 70*, 679–682.
5. Hasan, F., Shah, A. A., Javed, S., & Hameed, A. (2010). Enzymes used in detergents: lipases. *African Journal of Biotechnology, 9*(31), 4836–4844.
6. Sharma, D., Sharma, B., & Shukla, A. K. (2011). Biotechnological approach of microbial lipase: a review. *Biotechnology, 10*(1), 23–40.
7. Maynard, J. A., Chen, G., Georgiou, G., & Iverson, B. L. (2002). In vitro scanning-saturation mutagenesis. *Methods in Molecular Biology, 182*, 149–163.
8. Moreira, I. S., Fernandes, P. A., & Ramos, M. J. (2007). Computational alanine scanning mutagenesis—an improved methodological approach. *Journal of Computational Chemistry, 28*, 644–654.
9. Morrison, K. L., & Weiss, G. A. (2001). Combinatorial alanine-scanning. *Current Opinion in Chemical Biology, 5*, 302–307.
10. Gibbs, C. S., & Zoller, M. J. (1991). Identification of electrostatic interaction that determine the phosphorylation site specificity of the camp-dependent protein kinase. *Biochemistry, 30*, 5329–5334.
11. Blaber, M., Baase, W. A., Gassner, N., & Matthews, B. W. (1995). Alanine scanning mutagenesis of the alpha-helix 115–123 of phage T4 lysozyme: effects on structure, stability and the binding of solvent. *Journal of Molecular Biology, 246*, 317–330.
12. Pezzullo, M., Del Vecchio, P., Mandrich, L., Nucci, R., Rossi, M., & Manco, G. (2013). Comprehensive analysis of surface charged residues involved in thermal stability in *Alicyclobacillus acidocaldarius* esterase 2. *Protein Engineering Design and Selection, 26*(1), 47–58.
13. Timucin, E., & Sezerman, O. U. (2013). The conserved lid tryptophan, W211, potentiates thermostability and thermoactivity in bacterial thermoalkalophilic lipases. *PloS One, 8*(12), 1–17.
14. Gudiukaitė, R., Gegeckas, A., Kazlauskas, D., & Citavicius, D. (2014). Influence of N- and/or C-terminal regions on activity, expression, characteristics and structure of lipase from *Geobacillus* sp. 95. *Extremophiles, 18*(1), 131–145.
15. Sambrook, J., & Rusell, D. W. (2001). *Molecular cloning: a laboratory manual*. New York: Cold Spring Harbor Lab Press.
16. Crooks, G. E., Hon, G., Chandonia, J. M., & Brenner, S. E. (2004). WebLogo: a sequence logo generator. *Genome Research, 14*, 1188–1190.
17. Wiederstein, M., & Sippl, M. J. (2007). ProSA-web:interactive web service for the recognition of errors in three-dimensional structures of protein. *Nucleic Acids Research, 35*, 407–410.
18. Olechnovič, K., Kulberkytė, E., & Venclovas, Č. (2013). CAD-score: a new contact area difference-based function for evaluation of protein structural models. *Proteins, 81*(1), 149–162.
19. Laemmly, U. K. (1970). Cleavage of structural proteins during the assembly of the head of bacteriophage T4. *Nature, 227*, 380–685.
20. Leow, T. C., Rahman, R. N. Z. R. A., Basri, M., & Salleh, A. B. (2007). A thermoalkaliphilic lipase of *Geobacillus* sp. T1. *Extremophiles, 11*, 527–535.
21. Jiang, Y., Zhou, X., & Chen, Z. (2010). Cloning, expression, and biochemical characterization of a thermostable lipase from *Geobacillus stearothermophilus* JC. *World Journal of Microbiology and Biotechnology, 26*, 747–751.
22. Chakravorty, D., Parameswaran, S., Dubey, V. K., & Patra, S. (2011). In silico characterization of thermostable lipases. *Extremophiles, 15*(1), 89–103.
23. Carrasco-Lopez, C., Godoy, C., de las Rivas, B., Fernandez-Lorente, G., Palomo, J. M., Guisan, J. M., Fernandez-Lafuente, R., Martinez-Ripoll, M., & Hermoso, J. A. (2009). Activation of bacterial thermoalkalophilic lipases is spurred by dramatic structural rearrangements. *JBC, 284*(7), 4365–4372.

24. Tyndall, J. D. A., Sinchaikul, S., Fothergill-Gilmore, L. A., Taylor, P., & Walkinshaw, M. D. (2002). Crystal structure of a thermostable lipase from *Bacillus stearothermophilus* P1. *Journal of Molecular Biology, 323*, 859–869.
25. Abdul Rahman, M. Z., Salleh, A. B., Abdul Rahman, R. N., Abdul Rahman, M. B., Basri, M., & Leow, T. C. (2012). Unlocking the mystery behind the activation phenomenon of T1 lipase: a molecular dynamics simulations approach. *Protein Sciences, 21*(8), 1210–1221.
26. Goodarzi, N., Karkhane, A. A., Mirlohi, A., Tabandeh, F., Torktas, I., Aminzadeh, S., Yakhchali, B., Shamsara, M., & Ghafouri, M. A. (2014). Protein engineering of *Bacillus thermocatenulatus* lipase via deletion of the α5 helix. *Applied Biochemistry and Biotechnology, 174*(1), 339–351.
27. Jeong, S. T., Kim, H. K., Kim, S. J., Chi, S. W., Pan, J. G., Oh, T. K., & Ryu, S. E. (2002). Novel zinc-binding center and a temperature switch in the *Bacillus stearothermophilus* L1 lipase. *Journal of Biological Chemistry, 277*(19), 17041–17047.